Journal of Sound and Vibration (1986) **104**(3), 497-520

NON-LINEAR VIBRATORY INTERACTIONS IN SYSTEMS OF COUPLED BEAMS

S. L. BUX AND J. W. ROBERTS

Department of Mechanical Engineering, University of Edinburgh, Edinburgh EH9 3JL, Scotland

(*Received* 8 *February* 1984, *and in revised form* 27 *February* 1985)

Small non-linear interactions of the type referred to as autoparametric may have a considerable effect on the forced oscillatory behaviour of structures. Under conditions of internal resonance these effects may bring about complex forms of response where the normal linear resonance of a directly excited mode is absorbed, and indirectly excited modes show simultaneous large non-synchronous responses. In this paper the forced vibration of a system of coupled beams is examined and it is shown that violent non-synchronous torsion and bending vibration observed in such a system may be explained by the existence of quadratic non-linear coupling terms and internal resonance effects between three and four modes. A finite degree of freedom model was formulated and the method of multiple scales was applied. For the case of three-mode interactions stationary solutions were obtained which gave very satisfactory agreement with measured responses, and showed the effects of detuning of the internal resonance. The analysis also gave a clear indication of the cause of strong four-mode interactions but did not yield stationary solutions in this case. Experimental results are included to illustrate the four-mode interactive response.

1. INTRODUCTION

In many structural and machine vibration problems, contributions to the system kinetic energy arising from the geometry and deformation of the system lead to small quadratic and higher order non-linear terms in the system equations of motion. When an additional factor of internal resonance is present (i.e., critical relationships exist between values of the natural frequencies), these terms even when small may have significant effects on the system forced vibration response, such that gross departures from the usual patterns of linear response may be observed. It is possible for the linear resonance peak of a directly excited mode to be absorbed with an accompanying steady vibration in one or more indirectly excited modes at frequencies remote from the external excitation frequency. The responses are highly non-linear with respect to excitation level and show a complex pattern of amplitude jump and hysteresis effects. Regions of unsteady beating response are also observed.

Quadratic coupling terms in particular are frequently referred to as "autoparametric" because the form of these terms represents a situation where response in one mode appears as a parametric loading in a further mode. In general the subject is one of some mathematical complexity and has developed rapidly in recent years.

The present paper deals with the analysis of strong autoparametric interactions observed in a simple structural configuration consisting of two beams coupled at right angles (see Figure 1) with transverse external excitation on the primary beam *OB*. This model arrangement was used in a study of the autoparametric vibration problem of the two fundamental bending modes under random excitation [1] and was subsequently found to exhibit complex patterns of vibrational instability and energy flow. In-plane excitation

0022-460X/86/030497+24 $03.00/0

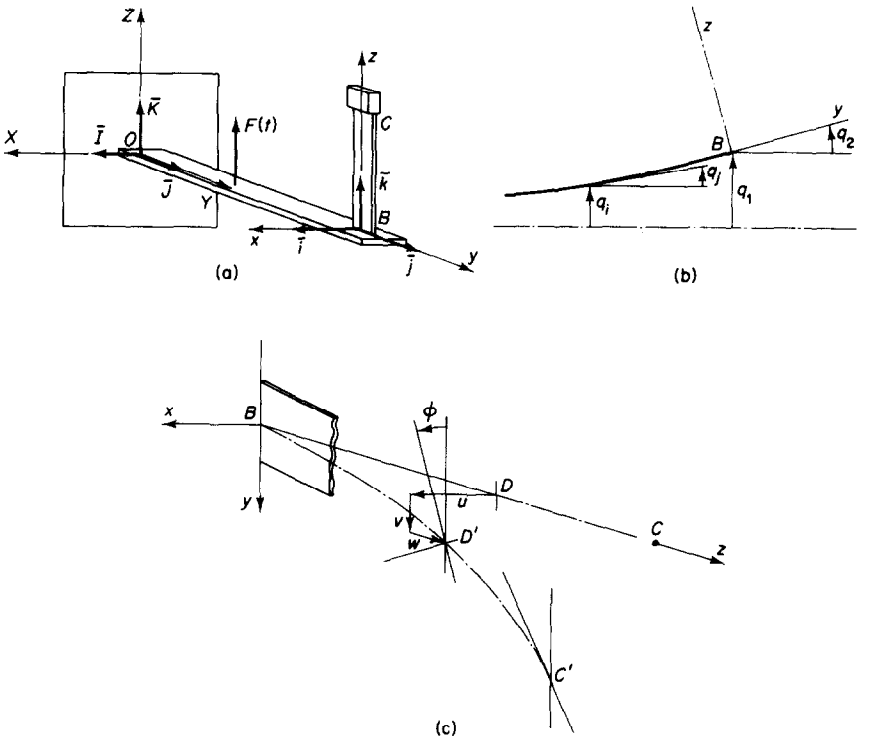

Figure 1. System configuration and deformation. (a) Layout and co-ordinate frames; (b) primary beam deformation co-ordinates; (c) secondary beam deformations.

in the region of the second in-plane bending resonance at 52 Hz was found to cause violent response of the first out-of-plane bending mode of the auxiliary beam *BC* at 4·5 Hz. Closer inspection revealed that torsional response of the beam *BC* was also present at 46 Hz and that occasionally there was also a steady accompanying vibration in the first in-plane mode at 9·5 Hz. An explanation for these responses has been found on the basis of two types of autoparametric interaction. First of all dynamic pitching at the coupling point due to in-plane bending may induce out-of-plane bending combined with torsion of the auxiliary beam as a combination type parametric instability, while the quadratic moment reaction on the primary beam absorbs the usual linear resonance peak. This effect requires proximity to the resonance conditions,

$$\Omega \simeq \omega_2 \simeq \omega_B + \omega_T, \tag{i}$$

the first part indicating external resonance with the second in-plane mode, and the second part indicating combination internal resonance of the second in-plane mode with the sum of first bending and torsion of the auxiliary beam. The second type of autoparametric interaction is a supplement to the first and involves a quadratic transverse reaction force term at the coupling point arising from the first out-of-plane bending motion also being resonant with the first in-plane bending mode and driving a first mode response. This effect will be significant under the resonance condition

$$\omega_1 \simeq 2\omega_B. \tag{ii}$$

Small non-linear coupling terms, magnified by the realization of conditions (i) and (ii), are the source of the observed complex vibrations.

In N degree of freedom systems internal resonance implies that the natural frequencies are commensurable, satisfying general forms

$$\sum_{i=1}^{n} k_i \omega_i = 0, \tag{iii}$$

where the k_i are integers, and effects of autoparametric coupling and internal resonances have been reported elsewhere. The subject is closely related to the problem of parametric excitation of bending and torsion of beams. Bolotin [2] has treated the principal parametric resonance in a simply-supported beam subjected to periodic end moments, and in a cantilever with an end mass subjected to a periodic load at the free end. More recently, the parametric combination resonance of a cantilever beam undergoing support motion has been considered by Dugundji and Mukhopadhyay [3], and by Dokumaci [4].

The classical example of an autoparametrically excited system is the elastic pendulum, which is capable of both longitudinal extension and swinging pendulum motion. This system has been extensively investigated and one such study was recently made by Breitenberger and Mueller [5]. It is now known that complex behaviour arises in the vicinity of exact internal resonance when the natural frequency of longitudinal motion is approximately twice the natural frequency of pendulum motion. A continuous exchange of energy occurs between the coupled motions resulting in amplitude modulated responses. The theoretical analysis of the effects of autoparametric resonance in non-autonomous systems was initially conducted by Sethna [6] for a two-degree-of-freedom system with one natural frequency twice the other. Recently, Yamamoto *et al.* [7, 8] extended the analysis to include both quadratic and cubic non-linearities, while Yamamoto *et al.* [9] studied a system with cubic and fourth order non-linearities and with natural frequencies in the ratio 2:3. Sethna and Bajaj [10] presented an analytical method to determine amplitude modulated motion in a two-degree-of-freedom system with quadratic non-linearities.

In recent physical applications, Haxton and Barr [11] examined a two-mode interaction response in an autoparametric vibration absorber. Barr and Nelson [12] considered a coupled beam system with internal resonance of the type $\omega_i = 2\omega_j$, as well as a combination type, that is, $\omega_i = \omega_j + \omega_k$, involving three modes. Nayfeh *et al.* [13] analyzed two-mode interaction behaviour in ships involving non-linear coupling between pitching and rolling motion. Mook *et al.* [14] extended the analysis to include both superharmonic and subharmonic resonances. In another application, Ibrahim and Barr [15, 16] investigated a structure-liquid system exhibiting both two- and three-mode interactions. The combination type internal resonance has also been observed in an excited piezo-electric crystal by Yen and Kronauer [17], and in a spinning nutating plate by Klahs and Ginsberg [18]. Hatwal *et al.* [19] have recently examined a two-degree-of-freedom autoparametric system and determined a second order approximation solution. By extending the analysis to include additional degrees of freedom, it is possible to generate multiple internal resonance conditions. Barr [20] has described the possibility of cascading interactions whereby one or more modes involved in one internal resonance condition also satisfy another separate internal resonance condition. This effect can propagate to involve multi-modal responses and, in this manner, modes not directly excited by the external disturbance can still respond significantly through the non-linear resonance coupling. Ibrahim [21] studied such multiple internal resonances in a structure-liquid system while Barr and Ashworth [22] examined multi-modal interactions in a fuselage-tail plane assembly model.

The coupled beam system considered here is represented as a finite degree-of-freedom model. The generalized equations of motion are derived up to second order by the method of Lagrange. These equations are then transformed to normal co-ordinates by assuming

a two-mode Galerkin approximation for the planar motion. The resulting system of non-linear ordinary coupled equations are analyzed by the method of multiple scales [23, 24]. This analysis is conducted for the case of external forced resonance of the second bending mode of the main beam, $\Omega = \omega_2$, in the presence of a single internal resonance condition, $\omega_2 = \omega_B + \omega_T$. Stationary solutions to the first order approximation are obtained. Comparisons with the theoretical predictions are provided by results from measurements of the experimental model response.

In the more complicated four-mode coupling case, the perturbation analysis shows clearly the significance of the multiple internal resonance conditions. An autonomous set of first order differential equations with respect to the slow time scale are derived for the modal amplitudes and phases in terms of the modal damping factors and detuning parameters. Stationary analytical solutions for these have not been obtained and the analysis as yet gives only a qualitative basis for understanding four-mode interactions. Experimental results are presented to show the four-mode coupling.

2. SYSTEM EQUATIONS OF MOTION

2.1. KINEMATICS

Figure 1(a) shows a schematic diagram of the beam system and co-ordinate frames. The primary beam is designated *OB* and the secondary beam of length l is designated *BC*. *B* is the coupling point. The external excitation is presumed to act in the *OZ* direction on the primary beam, and to be monofrequent. It is here indicated as a single discrete force. Alternative forms such as distributed dynamic force or prescribed motion of the beam supports could be substituted. To avoid the need for excessively complex co-ordinate descriptions, motion of the primary beam is only considered in the plane *OYZ*. Flexural motion in the *OXY* plane and torsional motion are thus considered small and non-resonant as a consequence of the system geometry and frequency ranges. The planar motion may be described, with an arbitrary discretization of the beam, by using a set of generalized co-ordinates q_i, $i = 1, \ldots, n$ (see Figure 1(b)). q_1 and q_2 are designated to specify the transverse displacement and planar rotation of the coupling point *B*. Furthermore, motion of the primary beam is presumed to be within the linear range of deflection and slope, and axial contraction effects are neglected.

For the secondary beam *BC* (see Figure 1(c)) it is presumed in the analysis that for the cross-section the shear centre and centroid coincide, and that for simplicity the beam is modelled as having a single discrete inertia element. Let u, v and w denote displacement functions of z and time t of the beam elastic axis in the x, y and z direction and let $\phi(z, t)$ denote the cross-section rotation; u_0, v_0, etc., are used to denote the corresponding values at the inertia element $z = l$. Continuity of motion at the coupling point implies that $q_1 \bar{K}$ is a displacement of *B* and that the frame *Bxyz* has a vector angular velocity given by $\dot{q}_2 \bar{I}$.

Two further equations of constraint are justified by the geometry of the system. First it is assumed that extension of the beam elastic axis is negligible. From geometrical considerations this leads to

$$w_0 = \int_0^l \tfrac{1}{2}[u'(z)^2 + v'(z)^2]\,\mathrm{d}z. \tag{1}$$

The second constraint is based on the beam cross-section being thin and blade-like in the plane *OYZ* such that the flexural rigidity for bending in one principal plane may be considered very large compared with that in the other. In general the principal curvatures κ_1, κ_2 and the torsion τ at any point on the elastic axis may be derived from the classical

theory of rods [25, 26]. These may be written to second order as

$$\kappa_1 = u''\phi - v'', \qquad \kappa_2 = u'' + v''\phi, \qquad \tau = \phi' + u''v' \tag{2-4}$$

(a prime denotes differentiation with respect to z). For $\kappa_1 \to 0$ one may assume, from equation (2),

$$v'' = u''\phi, \tag{5}$$

and hence, from geometrical considerations,

$$v_0 = \int_0^l (l-z)u''\phi \, \mathrm{d}z \tag{6}$$

to second order.

2.2. EQUATIONS OF MOTION

The foregoing equations of constraint together with assumed deformation modes

$$u(z, t) = f(z)u_0(t), \qquad \phi(z, t) = g(z)\phi_0(t), \tag{7, 8}$$

with $f(l) = g(l) = 1$, allow the motion of the coupled beam to be specified by two generalized co-ordinates u_0, ϕ_0. System equations of motion may be derived from Lagrangian considerations. In this, consideration is limited to energy terms up to cubic order. The resulting equations are

$$m_0\ddot{u}_0 + \lambda_1 u_0 = m\lambda_3 \ddot{q}_1 u_0 + m\lambda_4 l \ddot{q}_2 \phi_0, \tag{9}$$

$$I\ddot{\phi}_0 + \lambda_2 \phi_0 = m\lambda_4 l \ddot{q}_2 u_0. \tag{10}$$

In equations (9) and (10) $\lambda_1 - \lambda_4$ are integrals of the assumed deflection form functions given in Appendix I, m is the coupled beam discrete mass with polar inertia I, and m_0 is an equivalent mass such that $\frac{1}{2}m_0\dot{u}_0^2$ is the kinetic energy in a purely out-of-plane bending motion. The terms in $\ddot{q}_2\phi_0$ and $\ddot{q}_2 u_0$ represent coupled parametric excitation of torsion and non-planar bending of the secondary beam by planar rotational motion at the coupling point. The term $\ddot{q}_1 u_0$ in equation (9) represents direct parametric excitation of bending response of the secondary beam by transverse motion of the coupling point. The Lagrangian equations for the primary beam co-ordinates give equations of planar motion as

$$\underline{M}\ddot{\underline{q}} + \underline{K}\underline{q} = \underline{N}. \tag{11}$$

In (11) $\underline{K}$ is the stiffness matrix of the primary beam and incorporates support conditions. $\underline{M}$ is an augmented mass matrix such that $\frac{1}{2}\dot{\underline{q}}^{\mathrm{T}}\underline{M}\dot{\underline{q}}$ represents the whole system kinetic energy up to quadratic order in any purely planar motion ($u_0 = \phi_0 = 0$). $\underline{N}$ is a vector of generalized forces due to external excitation and non-linear interactive terms at the coupling point. In particular,

$$N_1 = m\lambda_3(\ddot{u}_0 u_0 + \dot{u}_0^2) + ml\ddot{q}_2^2, \tag{12}$$

$$N_2 = ml\lambda_4(\ddot{u}_0\phi_0 + 2\dot{u}_0\dot{\phi}_0 + u_0\ddot{\phi}_0). \tag{13}$$

N_1 is the interactive transverse force at the coupling point due to bending motion of the coupled beam, with a further term from the centripetal acceleration. N_2 is the reactive moment on the primary beam due to non-planar bending and torsion of the secondary beam. Finally the external excitation is here conveniently included as a single discrete force in co-ordinate q_k, giving

$$N_k = P_0 \cos \Omega t. \tag{14}$$

The basic system equations (9)-(14) show the presence of the quadratic non-linear interactions due to the system geometry. The equations may be further reduced by assuming a two-mode representation of the planar motion. One writes

$$q_i = \psi_{i1}\xi_1 + \psi_{i2}\xi_2, \tag{15}$$

where ψ_{ij} is the ith element of the jth eigenvector of the linearized undamped planar motion of the whole system. ξ_1 and ξ_2 are generalized co-ordinates of the two selected planar modes. Substituting this expression into equation (11) and using the orthogonality properties of the eigenvectors yields

$$M_j\ddot{\xi}_j + K_j\xi_j = \psi_{kj}P_0 \cos \Omega t + \psi_{1j}m\lambda_3(\ddot{u}_0u_0 + \dot{u}_0^2) + \psi_{2j}m\lambda_4 l(\ddot{u}_0\phi_0 + 2\dot{u}_0\dot{\phi}_0 + u_0\ddot{\phi}_0) + \psi_{1j}ml\sum_i^2\sum_j^2 \psi_{2i}\psi_{2j}\dot{\xi}_i\dot{\xi}_j, \qquad j = 1, 2. \tag{16}$$

M_j and K_j are the generalized mass and stiffness of the jth mode. The final terms in equation (16) arising from planar centripetal action may be shown to be of negligible interest in the present study and are discarded. Linear modal damping is introduced and equations (9), (10) and (16) are rewritten in terms of non-dimensional measures, selecting co-ordinate q_r as an observation location for planar response. Thus one obtains, for the two in-plane modes,

$$\ddot{Y}_1 + \omega_1^2 Y_1 = \varepsilon[\rho\mu_{11}(\ddot{X}_1X_1 + \dot{X}_1^2) + \mu_{21}(\ddot{X}_1X_2 + 2\dot{X}_1\dot{X}_2 + X_1\ddot{X}_2) - 2\zeta_1\omega_1\dot{Y}_1 + P_1 \cos \Omega t], \tag{17}$$

$$\ddot{Y}_2 + \omega_2^2 Y_2 = \varepsilon[\rho\mu_{21}(\ddot{X}_1X_1 + \dot{X}_1^2) + \mu_{22}(\ddot{X}_1X_2 + 2\dot{X}_1\dot{X}_2 + X_1\ddot{X}_2) - 2\zeta_2\omega_2\dot{Y}_2 + P_2 \cos \Omega t]. \tag{18}$$

The equation for non-planar bending of the coupled beam becomes

$$\ddot{X}_1 + \omega_B^2 X_1 = \varepsilon[\rho\kappa_{11}\ddot{Y}_1X_1 + \rho\kappa_{12}\ddot{Y}_2X_1 + \kappa_{21}\ddot{Y}_1X_2 + \kappa_{22}\ddot{Y}_2X_2 - 2\zeta_B\omega_B\dot{X}_1], \tag{19}$$

and that for torsion of the coupled beam

$$\ddot{X}_2 + \omega_T^2 X_2 = \varepsilon[\kappa_{21}\ddot{Y}_1X_1 + \kappa_{22}\ddot{Y}_2X_1 - 2\zeta_T\omega_T\dot{X}_2], \tag{20}$$

where the response co-ordinates are defined by

$$X_1 = u_0/L_0, \qquad X_2 = r\phi_0/L_0, \qquad Y_1 = (\psi_{r1}/L_0)\xi_1, \qquad Y_2 = (\psi_{r2}/L_0)\xi_2. \tag{21, 22}$$

L_0 is an arbitrary displacement reference. ε is a small parameter given by

$$\varepsilon = (\lambda_4/r)L_0, \qquad \text{where } r = [I/m_0]^{1/2}. \tag{23}$$

The other coefficients in equations (17)-(20) are given as follows:

$$\kappa_{11} = \frac{\psi_{11}}{\psi_{r1}}\frac{m}{m_0}, \quad \kappa_{12} = \frac{\psi_{12}}{\psi_{r2}}\frac{m}{m_0}, \quad \kappa_{21} = \frac{\psi_{21}}{\psi_{r1}}\frac{lm}{m_0}, \quad \kappa_{22} = \frac{\psi_{22}}{\psi_{r2}}\frac{lm}{m_0}, \quad \rho = \frac{\lambda_3 r}{B_4},$$

$$\mu_{11} = \psi_{11}\psi_{r1}\frac{m_0}{M}, \quad \mu_{12} = \psi_{12}\psi_{r2}\frac{m_0}{M_2}, \quad \mu_{21} = \psi_{21}\psi_{r1}\frac{m_0 l}{M_1}, \quad \mu_{22} = \psi_{22}\psi_{r2}\frac{m_0 l}{M_2},$$

$$\varepsilon P_j = \frac{\psi_{kj}\psi_{rj}}{M_jL_0}P_0. \tag{24}$$

At this stage it is expedient to reconsider the physical basis of the problem of interest in anticipation of further analysis, rather than proceed with a general analysis of the

equations as they stand. The problem under consideration is that forced vibration in the vicinity of resonance of the second in-plane bending mode is observed to cause violent non-synchronous out-of-plane bending and torsion response with a pronounced distortion of the normal linear resonance peak, and has further been observed to cause a visible first in-plane mode response. A qualitative explanation for these three- and four-mode interactions follows from inspection of the equations. Assume that the external frequency Ω is close to resonance with the second in-plane frequency ω_2 in equation (18). The large resonant response will cause a substantial pitching angular acceleration at the coupling point which will then appear as a symmetrically coupled parametric load in the secondary beam bending and torsion equations: i.e., the terms $\ddot{Y}_2 X_2$ in equation (19) and $\ddot{Y}_2 X_1$ in equation (20). It is known that such a loading may drive a combination type parametric instability of sum type when $\Omega \simeq \omega_B + \omega_T$, with each of the modes responding in the vicinity of its own natural frequency. If these resonance conditions are satisfied it will then be the case that the quadratic reaction moment terms with coefficient μ_{22} in equation (18) will have a strong frequency content at $(\omega_B + \omega_T) \simeq \omega_2$ and will have a substantial influence on the planar response. Strong three-mode interactive responses are thus a consequence of the external and internal resonance condition

$$\Omega \simeq \omega_2 \simeq \omega_B + \omega_T. \tag{25}$$

Further inspection of the equations reveals the source of the observed four-mode interactions. In equation (17) the quadratic terms in $\ddot{X}_1 X_1$, etc., with coefficient $\rho\mu_{11}$, represent a transverse force at the coupling point arising from the out-of-plane bending response. This effect will be resonant with the first in-plane mode if the additional internal resonance condition is realized,

$$2\omega_B \simeq \omega_1, \tag{26}$$

in which case first planar mode response will accompany the three-mode interaction. Simultaneously the quadratic coupling term in $\ddot{Y}_1 X_1$ in equation (19) will have resonant content at ω_B and will contribute to the non-planar bending mode response. It may be reasonably assumed that the other quadratic terms in the equations are non-resonant and play no significant part in the interactive motions, and will be discarded to avoid unnecessary algebra. Similarly the external forcing term in equation (17) may be regarded as far from resonance and insignificant. The reduced equations for consideration are thus

$$\ddot{Y}_1 + \omega_1^2 Y_1 = \varepsilon[\rho\mu_{11}(\ddot{X}_1 X_1 + \dot{X}_1^2) - 2\zeta_1\omega_1 \dot{Y}_1], \tag{27}$$

$$\ddot{Y}_2 + \omega_2^2 Y_2 = \varepsilon[\mu_{22}(\ddot{X}_1 X_2 + 2\dot{X}_1 \dot{X}_2 + X_1 \ddot{X}_2) - 2\zeta_2\omega_2 \dot{Y}_2 + P\cos\Omega t], \tag{28}$$

$$\ddot{X}_1 + \omega_B^2 X_1 = \varepsilon[\rho\kappa_{11} \ddot{Y}_1 X_1 + \kappa_{22} \ddot{Y}_2 X_2 - 2\zeta_B\omega_B \dot{X}_1], \tag{29}$$

$$\ddot{X}_2 + \omega_T^2 X_2 = \varepsilon[\kappa_{22} \ddot{Y}_2 X_1 - 2\zeta_T\omega_T \dot{X}_2]. \tag{30}$$

These represent the four-mode problem. The more elementary case of three-mode interaction is obtained by setting $Y_1 = 0$.

3. RESPONSE ANALYSIS

3.1. MULTIPLE SCALES SOLUTION

The solution process used is the method of multiple scales [23], which has been widely applied to a number of non-linear oscillatory problems [24] where exact solutions are not possible. Solution will be sought to first order. Two time scales are introduced:

$$T_0 \equiv t, \qquad T_1 \equiv \varepsilon t. \tag{31}$$

Derivatives with respect to t are then transformed as

$$d/dt = \partial/\partial T_0 + \varepsilon \partial/\partial T_1 = D_0 + \varepsilon D_1, \qquad d^2/dt^2 = D_0^2 + 2\varepsilon D_0 D_1. \tag{32, 33}$$

The solution of equations (27)-(30) is assumed to be of the following form, with analogous expansions for X_2, Y_1, Y_2,

$$X_1(t, \varepsilon) = X_{10}(T_0, T_1) + \varepsilon X_{11}(T_0, T_1). \tag{34}$$

Substituting these expressions into equations (27)-(30) and equating coefficients of like powers of ε gives, for ε^0,

$$D_0^2 Y_{10} + \omega_1^2 Y_{10} = 0, \qquad D_0^2 Y_{20} + \omega_2^2 Y_{20} = 0, \qquad D_0^2 X_{10} + \omega_B^2 X_{10} = 0,$$
$$D_0^2 X_{20} + \omega_T^2 X_{20} = 0, \tag{35}$$

and for ε^1,

$$D_0^2 Y_{11} + \omega_1^2 Y_{11} = -2D_0 D_1 Y_{10} - 2\zeta_1 \omega_1 D_0 Y_{10} + \rho \mu_{11} \{X_{10} D_0^2 X_{10} + (D_0 X_{10})^2\}, \tag{36a}$$

$$D_0^2 Y_{21} + \omega_2^2 Y_{21} = -2D_0 D_1 Y_{20} + P \cos \Omega T_0 - 2\zeta_2 \omega_2 D_0 Y_{20}$$
$$+ \mu_{22} \{X_{20} D_0 X_{10} + 2D_0 X_{10} D_0 X_{20} + X_{10} D_0^2 X_{20}\}, \tag{36b}$$

$$D_0^2 X_{11} + \omega_B^2 X_{11} = -2D_0 D_1 X_{10} - 2\zeta_B \omega_B D_0 X_{10} + \rho \kappa_{11} X_{10} D_0^2 Y_{10} + \kappa_2 X_{20} D_0^2 Y_{20}, \tag{36c}$$

$$D_0^2 X_{21} + \omega_T^2 X_{21} = -2D_0 D_1 X_{20} - 2\zeta_T \omega_T D_0 X_{20} + \kappa_{22} X_{10} D_0^2 Y_{20}. \tag{36d}$$

General solutions of equations (35) may be written in the form

$$Y_{10} = B_1(T_1) \exp(i\omega_1 T_0) + cc, \qquad Y_{20} = B_2(T_1) \exp(i\omega_2 T_0) + cc, \tag{37a, b}$$

$$X_{10} = A_1(T_1) \exp(i\omega_B T_0) + cc, \qquad X_{20} = A_2(T_1) \exp(i\omega_T T_0) + cc, \tag{37c, d}$$

where B_1, etc., are complex functions of slow time T_1 and cc denotes complex conjugate. These may be substituted into equations (36) to yield equations for the first order perturbations. These are not solved explicitly. However the requirement for boundedness of the solutions, that secular or resonant terms be eliminated from the right-hand sides of (36a)-(36d), leads to a set of first order differential equations in T_1 for the complex response amplitudes A_1, etc. The forms of these solvability conditions depends on the resonance conditions which exist and these are considered separately.

3.2. THREE-MODE INTERACTIONS

The form of the solvability conditions is found to be affected substantially by the existence of an internal resonance condition between three modes, written formally as

$$\omega_2 = \omega_B + \omega_T + \varepsilon \sigma_1, \tag{38}$$

together with external resonance with the second planar mode, written as

$$\Omega = \omega_2 + \varepsilon \sigma. \tag{39}$$

In equations (38) and (39) σ and σ_1 are detuning parameters.

Upon introducing polar forms for the complex amplitudes,

$$A_1 = (a_1/2) \exp(i\alpha_1), \qquad A_2 = (a_2/2) \exp(i\alpha_2), \qquad B_2 = (b_2/2) \exp(i\beta_2), \tag{40a-c}$$

and the modified phase variables

$$\gamma_1 = \sigma T_1 - \beta_2, \qquad \gamma_2 = \sigma_1 T_1 - \alpha_1 - \alpha_2 + \beta_2, \tag{41}$$

solvability conditions are obtained as the autonomous set

$$\omega_2 b_2' = -\zeta_2 \omega_2^2 b_2 + (\mu_{22}/4)(\omega_B + \omega_T)^2 a_i a_2 \sin \gamma_2 + (P/2) \sin \gamma_1, \tag{42a}$$

$$\omega_2 b_2 \gamma_1' = \omega_2 \sigma b_2 - (\mu_{22}/4)(\omega_B + \omega_T)^2 a_1 a_2 \cos \gamma_2 + (P/2) \cos \gamma_1, \tag{42b}$$

$$\omega_B a_1' = -\zeta_B \omega_B^2 a_1 - (\kappa_{22}/4)\omega_2^2 a_2 b_2 \sin \gamma_2, \tag{42c}$$

$$\omega_T a_2' = -\zeta_T \omega_T^2 a_2 - (\kappa_{22}/4)\omega_2^2 a_1 b_2 \sin \gamma_2, \tag{42d}$$

$$a_1 a_2 \omega_B \omega_T (\gamma_1 + \gamma_2)' = \omega_B \omega_T (\sigma + \sigma_1) a_1 a_2 - (\kappa_{22}/4)\omega_2^2 (\omega_B a_1^2 + \omega_T a_2^2) b_2 \cos \gamma_2. \tag{42e}$$

Stationary solutions to the system equations (27)-(30) may be explored by setting the derivatives with respect to T_1 equal to zero. (This does not preclude the possibility of non-stationary solutions of equations (42) and indeed non-stationary responses are observed frequently in the physical model.) The equations (42) are then seen to admit, first of all, the purely in-plane solution

$$a_1 = a_2 = 0, \; b_2 \neq 0, \tag{43}$$

and one obtains

$$b_2 = P/2\omega_2[\sigma^2 + \zeta_2^2 \omega_2^2]^{1/2}, \qquad \tan \gamma_1 = -\zeta_2 \omega_2 / \sigma. \tag{44}$$

This represents the linear forced resonance of the second in-plane mode.

For the general case, upon assuming $a_1, a_2 \neq 0$, the following stationary solution is obtained after some manipulation. For the in-plane motion,

$$b_2 = (4\omega_B \omega_T / \kappa_{22} \omega_2^2) \sqrt{\zeta_B \zeta_T} \sqrt{1 + (\sigma + \sigma_1)^2 / (\zeta_B \omega_B + \zeta_T \omega_T)^2}. \tag{45}$$

For bending of the secondary beam,

$$a_1^2 = [2/\mu_{22}(\omega_B + \omega_T)^2] \sqrt{\zeta_T \omega_T^2 / \zeta_B \omega_B^2} \, [-L_1 \pm \sqrt{P^2 - L_2^2}], \tag{46}$$

with

$$L_1 = [8\sqrt{\zeta_B \omega_B^2 \zeta_T \omega_T^2} / \kappa_{22}(\zeta_B \omega_B + \zeta_T \omega_T)\omega_2][\zeta_2 \omega_2 (\zeta_B \omega_B + \zeta_T \omega_T) - \sigma(\sigma + \sigma_1)], \tag{47}$$

$$L_2 = [8\sqrt{\zeta_B \omega_B^2 \zeta_T \omega_T^2} / \kappa_{22}(\zeta_B \omega_B + \zeta_T \omega_T)\omega_2][(\zeta_B \omega_B + \zeta_T \omega_T)\sigma + \zeta_2 \omega_2 (\sigma + \sigma_1)], \tag{48}$$

and for torsion of the secondary beam,

$$a_2 = \sqrt{\zeta_B \omega_B^2 / \zeta_T \omega_T^2} \, a_1. \tag{49}$$

Expressions (45)-(49) represent the stationary three-mode interactive forced vibration response due to the non-linear coupling in terms of the system parameters (damping, detuning), etc. The responses in a_1 and a_2 are clearly non-synchronous from equation (37) being at frequencies close to the individual resonant frequencies. The form of equation (46) indicates that a_1 may have zero, one or two real non-zero solutions, and these are mirrored by a_2. It is necessary to examine the stability or otherwise of the stationary solutions to determine actual system behaviour. Stability is investigated by the standard technique of adding a perturbation to the solutions and determining the eigenvalues of the five by five matrix of the resultant linearized system. The elements of the system matrix are given in Appendix II. Stability may only be determined for specific numerical values but calculations generally indicate that when a single real non-planar solution exists it is stable, but when two real solutions are obtained the smaller is unstable.

3.3. THEORETICAL RESPONSE CURVES

The response of the externally excited mode b_2 given by equation (45) shows that the amplitude is independent of external excitation level. This is a saturation phenomenon which is a characteristic feature of autoparametrically excited systems with quadratic

non-linearities satisfying the simpler internal resonance relationship $\omega_1 = 2\omega_2$, when excited at the higher natural frequency. The response is also unaffected by primary system damping. There is a simple relationship for locating the point of minimum response. The term $1+(\sigma+\sigma_1)^2/(\zeta_B\omega_B+\zeta_T\omega_T)^2 \geqslant 1$, so that the minimum always occurs when $\sigma+\sigma_1=0$ or $\sigma_1=-\sigma_1$. This implies the point of minimum response is determined solely by the amount of internal detuning. The response of the coupled beam modes a_1 and a_2 are given by equations (46)-(49). Equation (49) indicates that the ratio of their response values, a_1/a_2, is governed by two ratios, these being the ratio of the coupled system damping, ζ_T/ζ_B, and the ratio of the coupled system natural frequencies, ω_T/ω_B. This result reflects an analogous feature of combination resonances in parametrically excited systems.

Typical responses are depicted in Figures 2(a)-(c) for an excitation amplitude $P=15$. As the external frequency is increased from below and reaches point B, the in-plane solution ($a_1=a_2=0$ in Figures 2(b) and (c)) becomes unstable, and a jump in response occurs from B to B'. At the same time the linear forced response of b_2 becomes unstable with the response following the non-linear response curve BFC. It is noted that point B is exactly coincident with both the linear forced resonance curve and the non-linear response curve of b_2. With increasing external detuning, the response curves of all three modes decrease to a minimum value at $\sigma=0$, beyond which the response increases again until point C, where real solutions to a_1 and a_2 cease to exist. Here a downward jump in response occurs with the b_2 mode returning to the linear forced response and the a_1 and a_2 modes returning to the zero solution. For exact internal resonance the response curves are symmetric about the $\sigma=0$ axis. Therefore, a reversal of the response pattern occurs with initial excitation frequency at point E and decreasing external detuning. The response of b_2 follows $EFBGA$, while a_1 and a_2 follow $EFF'G'A$. Introducing a finite amount of internal detuning causes an asymmetry of the response curves as shown by $NJMK$ for b_2 in Figure 2(a), and $JNJ'M'KM$ for a_1 and a_2 in Figures 2(b) and (c). The response sequence follows in a similar order as indicated by the arrows.

The system response can also be conveniently studied for a fixed value of the external detuning parameter σ while varying the excitation parameter P. When one starts at point A in Figure 3(a), and increases the force amplitude, P, then b_2 responds according to its linear resonance solution. On reaching point B, the zero solutions of a_1 and a_2 (see Figures 3(b) and (c)) are unstable and a jump in response occurs from B to B'. The linear response of the b_2 mode, BH, is unstable and the response follows BC instead, while a_1 and a_2 follow $B'C'$. At points C and C', if the force amplitude is decreased, the response retraces the BC and BC' curves and continues to points D and D', beyond which there are no real solutions for a_1 and a_2. A downward jump occurs with b_2 resuming the linear forced response while a_1 and a_2 return to their zero response solutions. The saturation phenomenon of the non-linear b_2 mode response as discussed earlier is clearly identifiable in Figure 3(a). The presence of oscillation hysteresis in the system response is also noted. Under exact external resonance, the response changes qualitatively. The threshold force amplitude at which autoparametric resonance begins is reduced. There is now no discontinuous change in a_1 and a_2. Instead the responses show a gradual increase when P is increased according to FG in Figures 3(b) and (c). When P is decreased the responses retrace the same paths from point G.

The effect of increasing or decreasing the external frequency through the resonance region with the accompanying jump phenomena has been described. It is also seen from the response curves that there are regions of the frequency axis where both the linear in-plane solution and the non-linear interactive solutions are stable, and the system motion may revert to either condition as a result of an impulse.

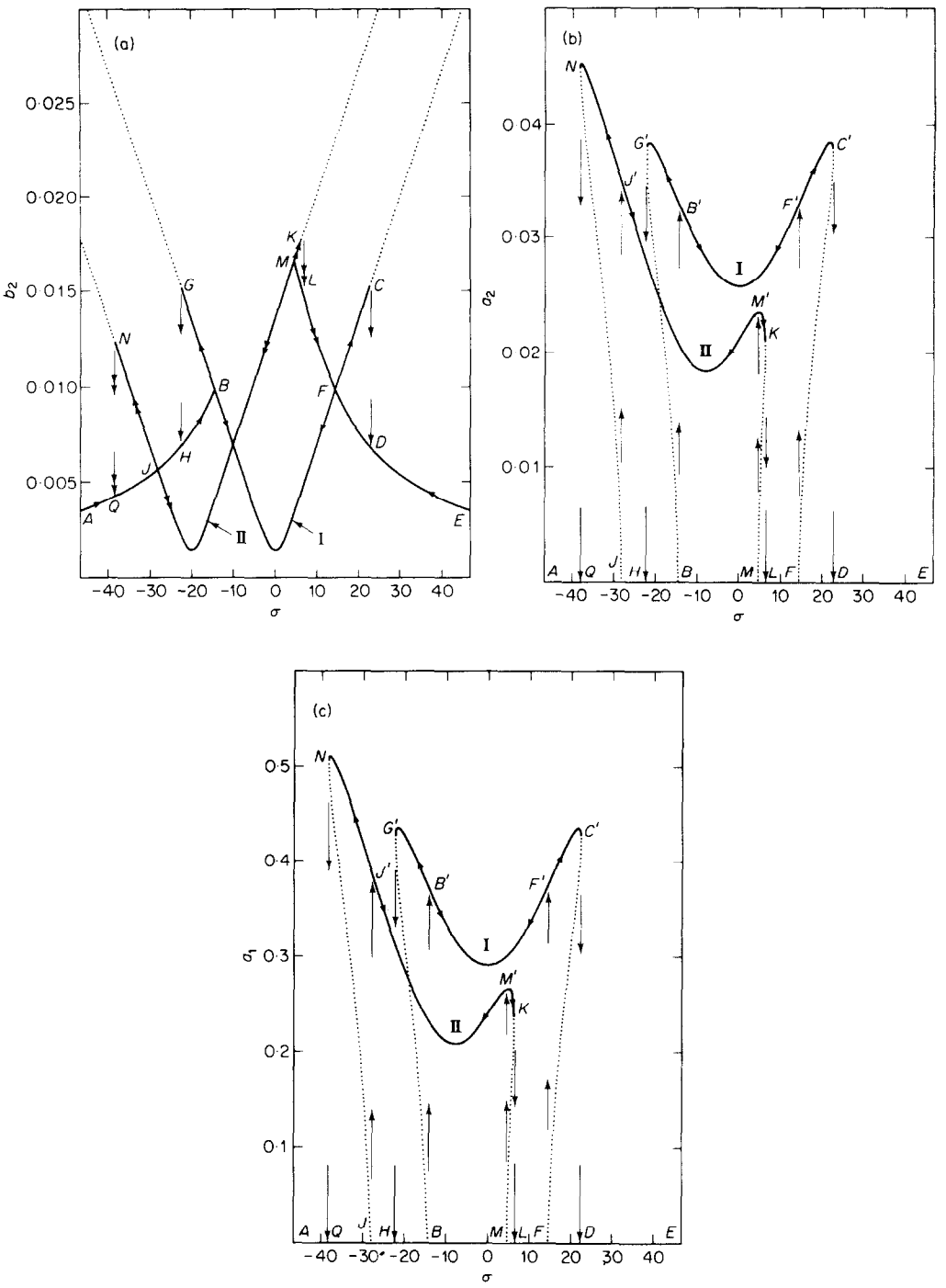

Figure 2. Theoretical stationary response amplitudes of system for three mode interactive motion under internal resonance condition ($\omega_2 = \omega_B + \omega_T + \varepsilon\sigma_1$) as functions of external detuning parameter σ ($\Omega = \omega_2 + \varepsilon\sigma$). $\varepsilon = 0{\cdot}075$, $P = 15$, $\zeta_B = \zeta_T = 0{\cdot}1$, $\zeta_2 = 0{\cdot}05$. For curves I $\sigma_1 = 0$; for curves II $\sigma_1 = 20$. (a) Planar second bending mode; (b) first torsional mode; (c) first non-planar bending mode. Dotted segments indicate unstable solutions.

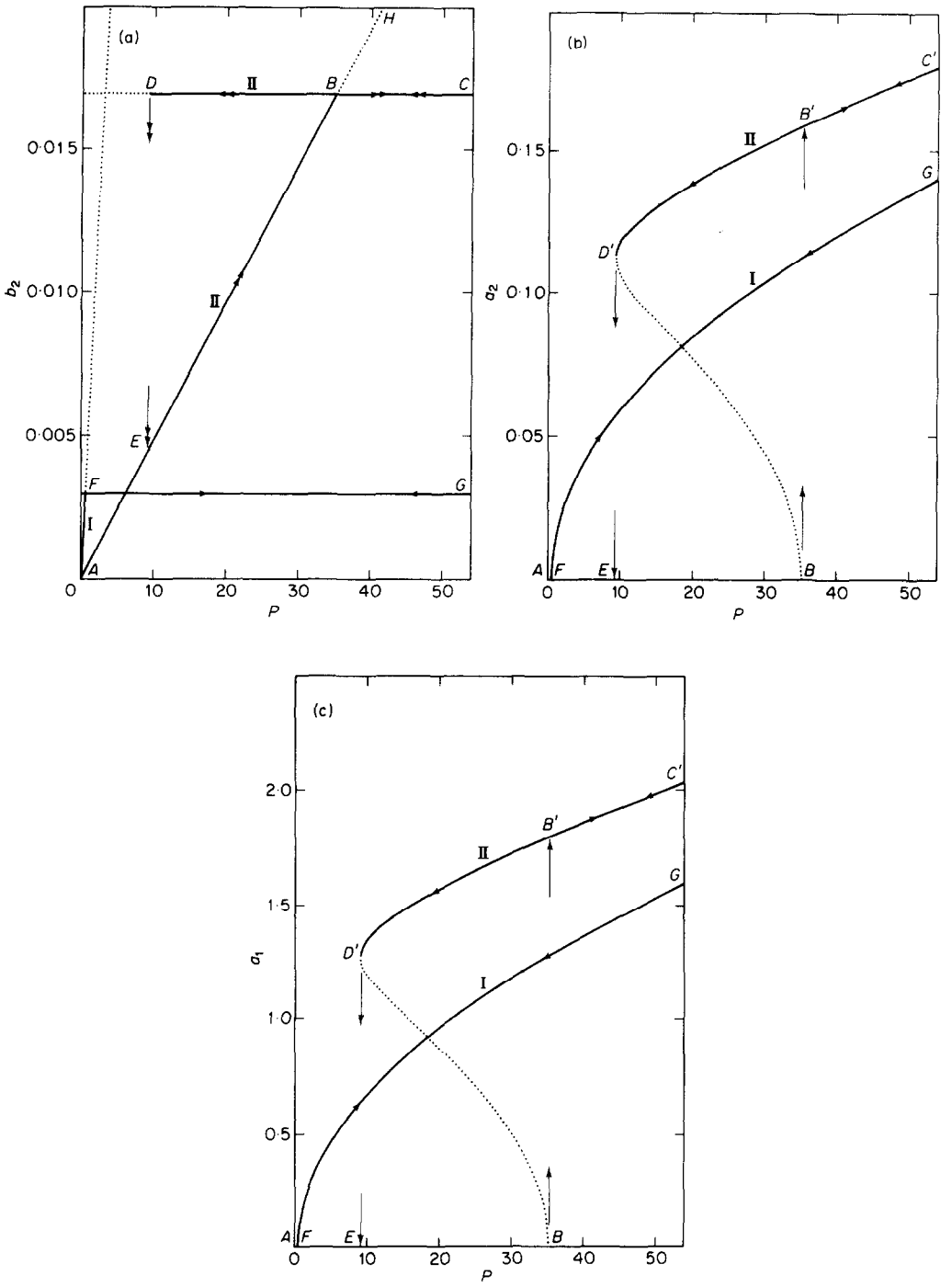

Figure 3. Theoretical stationary response amplitudes under internal resonance condition ($\omega_2 = \omega_B + \omega_T + \varepsilon\sigma_1$) as functions of excitation amplitude P. $\varepsilon = 0{\cdot}075$, $\sigma_1 = 0$, $\zeta_B = \zeta_T = 0{\cdot}1$, $\zeta_2 = 0{\cdot}05$. For curves I $\sigma = 0$; for curves II $\sigma = 25$. (a) Planar second bending mode; (b) first torsional mode; (c) first non-planar bending mode. Dotted segments indicate unstable solutions.

3.4. FOUR-MODE INTERACTIONS

When an additional internal resonance relation is admitted between the first in-plane mode and the out-of-plane bending mode, of the form

$$\omega_1 = 2\omega_B + \varepsilon\sigma_2, \tag{50}$$

four solvability conditions are obtained involving all three detuning parameters. As previously, these may be reduced to an autonomous set of first order equations in the four modal amplitudes, including the first in-plane mode response,

$$B_1(T_1) = (b_1(T_1)/2) \exp i\beta_1(T_1). \tag{51}$$

As in equation (41) an additional phase variable is introduced,

$$\gamma_3 = \sigma_2 T_1 + \beta_1 - 2\alpha_1, \tag{52}$$

and the following set of equations in slow time T_1 determine the first order solution to the system response:

$$\omega_1 b_1' = -\zeta_1\omega_1^2 b_1 + \tfrac{1}{2}\rho\mu_{11}\omega_B^2 a_1^2 \sin\gamma_3 \tag{53}$$

$$\omega_1\omega_B a_1 b_1 \gamma_3' = \omega_B\omega_1\sigma_2 a_1 b_1 - \tfrac{1}{2}\rho\kappa_{11}\omega_1^3 a_1 b_1^2 \cos\gamma_3 - \tfrac{1}{4}\kappa_{22}\omega_2^2\omega_1 a_2 b_1 b_2 \cos\gamma_2 + \tfrac{1}{2}\rho\mu_{11}\omega_B^3 a_1^3 \cos\gamma_3, \tag{54}$$

$$\omega_2 b_2' = -\zeta_2\omega_2^2 b_2 + \tfrac{1}{4}\mu_{22}(\omega_B + \omega_T)^2 a_1 a_2 \sin\gamma_2 + \tfrac{1}{2}P \sin\gamma_1, \tag{55}$$

$$\omega_2 b_2 \gamma_1' = \omega_2\sigma b_2 - \tfrac{1}{4}\mu_{22}(\omega_B + \omega_T)^2 a_1 a_2 \cos\gamma_2 + \tfrac{1}{2}P \cos\gamma_1, \tag{56}$$

$$\omega_B a_1' = -\zeta_B\omega_B^2 a_1 - \tfrac{1}{4}\rho\kappa_{11}\omega_1^2 a_1 b_1 \sin\gamma_3 - \tfrac{1}{4}\kappa_{22}\omega_2^2 a_2 b_2 \sin\gamma_2, \tag{57}$$

$$\omega_T a_2' = -\zeta_T\omega_T^2 a_2 - \tfrac{1}{4}\kappa_{22}\omega_2^2 a_1 b_2 \sin\gamma_2, \tag{58}$$

$$\omega_B\omega_T a_1 a_2(\gamma_1 + \gamma_2)' = \omega_B\omega_T(\sigma + \sigma_1) a_1 a_2 - \tfrac{1}{4}\kappa_{22}\omega_2^2(\omega_B a_1^2 + \omega_T a_2^2) b_2 \cos\gamma_2 - \tfrac{1}{4}\rho\kappa_{11}\omega_1^2 a_1 a_2 b_1 \cos\gamma_3. \tag{59}$$

While it is clear from the form of these that there will be additional interaction between the b_1 mode and the others as a consequence of multiple internal resonance it was not possible to obtain stationary solutions to the four mode equations by analysis, nor by a numerical approach, except for the unrealistic case of negligible damping [25]. These solutions are not discussed here.

4. EXPERIMENTAL INVESTIGATION

4.1. APPARATUS

The mechanical model used for experimental tests consisted principally of two steel beams of narrow rectangular cross-section, connected perpendicularly to one another as in Figure 1. The primary beam of dimensions 390 mm × 25·4 mm × 3·19 mm had one end clamped horizontally to a concrete worktable. The secondary beam of dimensions 154 mm × 19 mm × 0·47 mm was attached vertically to the free end of the primary beam by means of two right angle support brackets, arranged such that its bending displacement was perpendicular to the plane of the primary beam flexure as indicated in Figure 1. An adjustable mass in the form of a split and grooved steel block of total mass 46 g was attached to the secondary beam to allow adjustment of system natural frequencies. External excitation was provided by an electrodynamic vibrator connected to the primary beam at a distance of 80 mm from the clamped end. The vibrator connection was arranged to

have high axial stiffness but low flexural stiffness. Primary beam motion was monitored by means of an accelerometer attached to the beam at the point of application of the external excitation. The non-planar motion of the secondary beam, consisting of both bending and torsional displacements, was monitored by bending and shear strain gauges mounted near the clamped end of the beam. The linear natural frequencies and damping factors of the participating modes were determined by standard means, and the mass adjustment allowed tuning of the single or combined internal resonance condition. Eigenvector elements for the various modes were determined from a PAFEC finite element analysis.

The electrodynamic vibrator was powered by an amplifier with feedback current control which ensured that a constant current level and hence a constant force was supplied to the vibrator armature independent of the beam motion. The system behaviour was investigated by increasing and decreasing frequency through the region of forced resonance of the beam system. Testing was also conducted by keeping the excitation frequency constant and varying the excitation amplitude level. The transducer signals from the bending and torsion gauges and from the accelerometer measuring the primary beam response were monitored on a Hewlett Packard HP 3582A real time spectrum analyzer which was able to display a continuously updated spectrum of each of the input signals. The spectrum analyzer was particularly valuable as the frequency content of complicated waveforms was immediately identifiable.

4.2. GENERAL DISCUSSION OF RESULTS

A feature of the experimental model was that the tuning mass position could be adjusted to achieve the three-mode resonance condition (38) over a range of position, while over a narrow portion of that range the second internal resonance condition could also be achieved simultaneously. As a result it was found on exploring the range of model response that a wide variety of types of response could be obtained, varying from synchronous planar response at low excitation levels in the detuned condition to violent and irregular interactive motion at high excitation levels under critically tuned conditions. In attempting to correlate experimental results with the predicted stationary solutions, problems arose in categorizing transducer signals as stationary or otherwise. Generally speaking, for both three- and four-mode interactive motion at low levels of excitation, signals were reasonably stationary in the sense that the displayed spectra were single-peaked with at worst a small long-period fluctuation. It was noticeable however that torsional responses were frequently less stationary in appearance than bending responses for the same conditions. At high levels of excitation responses generally became visibly non-stationary by developing short period modulations and ultimately became very irregular. Because of the enormous variety of these responses and the wide range of system tuning and excitation conditions the results presented here are restricted to low excitation cases for which the interpretation of responses as stationary was reasonable and for which correlation with the stationary solution was possible. Further results have been presented in reference [26] but a systematic study of non-stationary regions of system behaviour remains to be carried out.

4.3. DISCUSSION OF RESULTS FOR THREE-MODE INTERACTIVE RESPONSE

Typical measurements of system response as functions of external detuning parameter σ are shown in Figures 4(a)-(c), 5(a)-(c) and 6(a)-(c) for three values of excitation amplitude P. The experimental results are shown as discrete points and no distinction is made between measured values for increasing and decreasing external detuning parameter σ. A typical test run starts with negative detuning and progresses through the

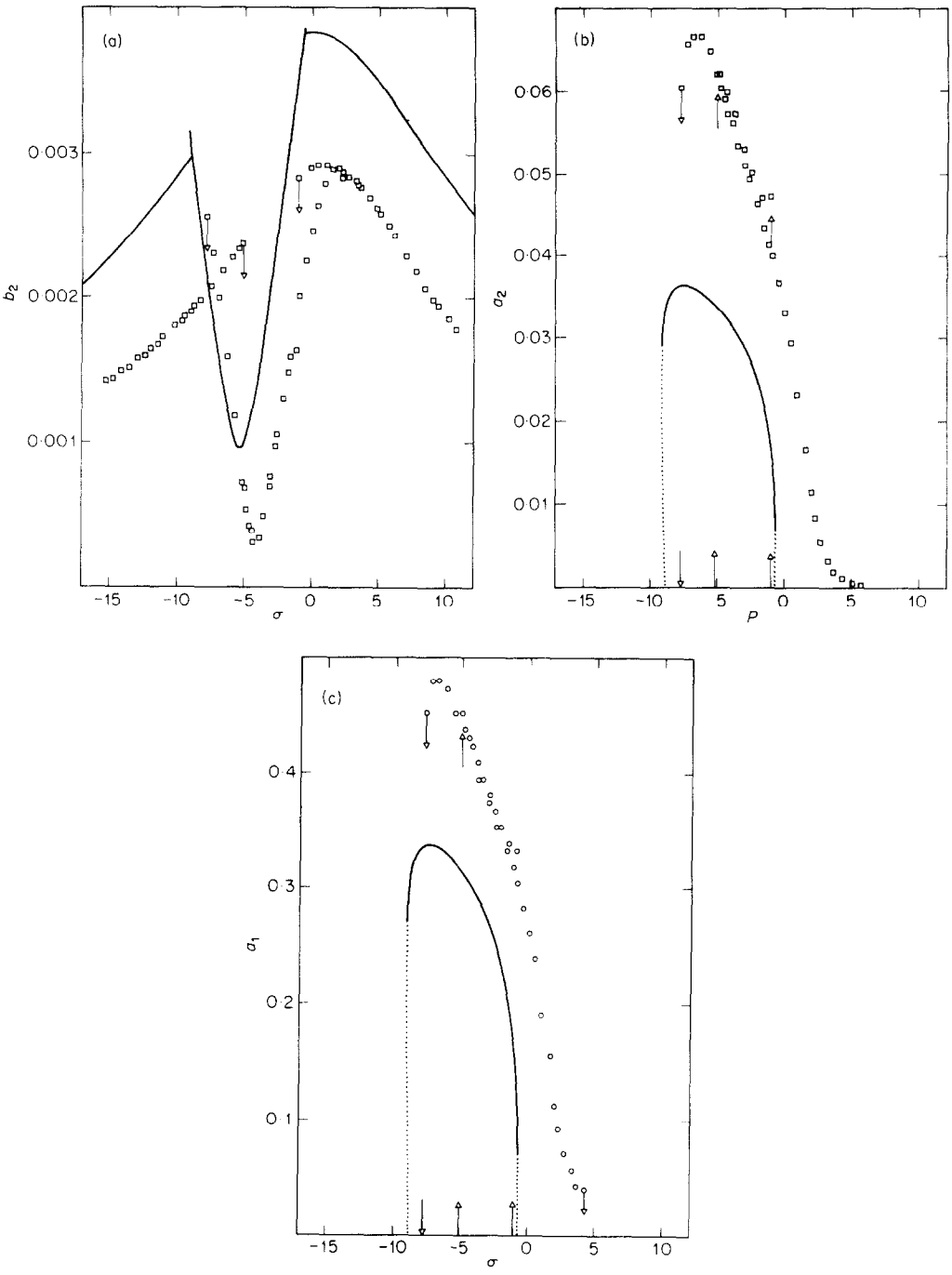

Figure 4. System three-mode interactive response amplitudes under internal resonance condition ($\omega_2 = \omega_B + \omega_T + \varepsilon\sigma_1$). $\varepsilon = 0{\cdot}075$, $P = 3{\cdot}8$, $\sigma_1 = 5{\cdot}3$, $\zeta_B = 0{\cdot}04$, $\zeta_T = 0{\cdot}03$, $\zeta_2 = 0{\cdot}27$. (a) Planar second bending mode; (b) first torsional mode; (c) First non-planar bending mode. ——, Theory; ⊡, experiment.

autoparametric resonance region to some positive value of σ for which the interactive motion has ceased. The onset of the resonance region is shown by the downward "jump" arrows for b_2 and upward "jump" arrows for a_1 and a_2. b_2 is the externally excited second planar bending mode while a_1 and a_2 are the parametrically excited non-planar torsion

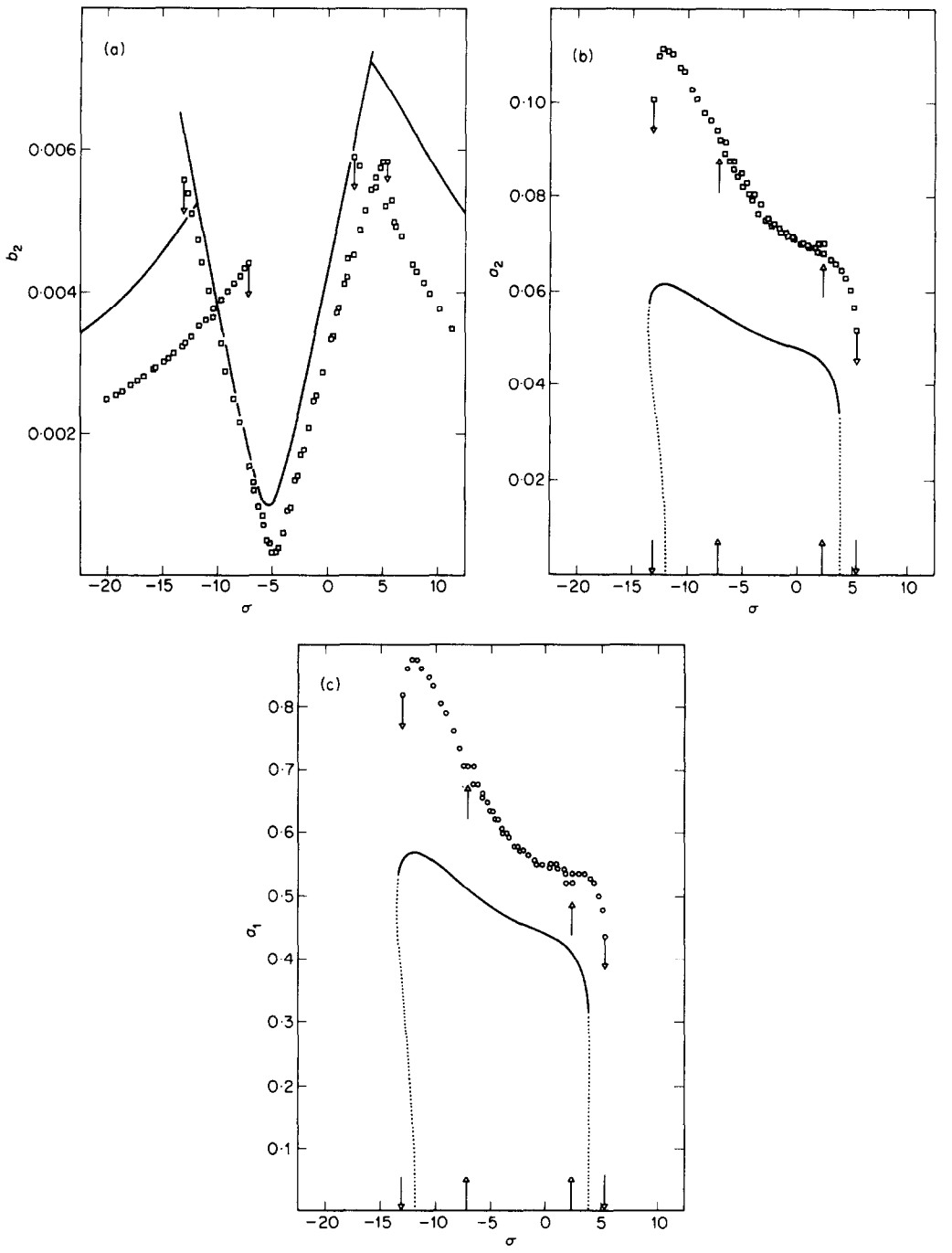

Figure 5. As for Figure 4 but with excitation parameter $P = 7{\cdot}6$.

and bending modes. The point at which autoparametric resonance stops is shown by the downward "jump" arrows for b_2, a_1 and a_2.

In Figures 4 and 5 there is very reasonable agreement, both qualitatively and quantitatively, between measured values and predicted responses. Generally the theoretical curves for b_2 are higher than the experimental values, while the non-planar modes a_1 and a_2

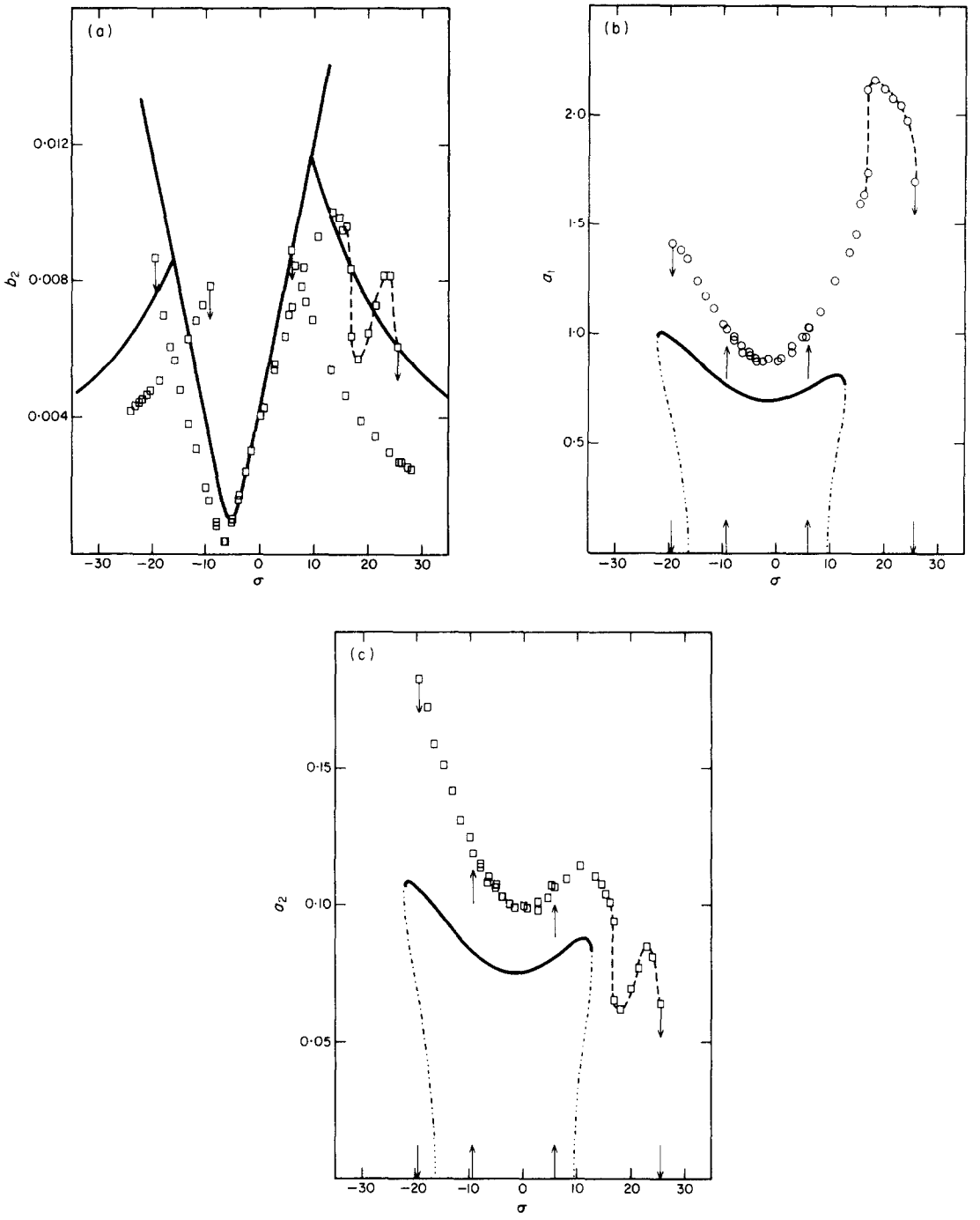

Figure 6. As for Figure 4 but with excitation parameter $P = 15$. Multi-harmonic response, —⊡—.

show the measured response to be higher than the predicted values. The region of autoparametric resonance measured in the model tends to be wider than the predicted regions. However, the measured points of instability of the zero solution of a_1 and a_2 are generally narrower than the corresponding theoretical points.

In contrast, Figure 6 gives results for a much higher level of excitation parameter P and reveals an onset of substantial departures from the predicted stationary response for each mode. There is an irregular extension of the autoparametric resonance region at its high frequency end with a considerable increase in the non-planar bending modal

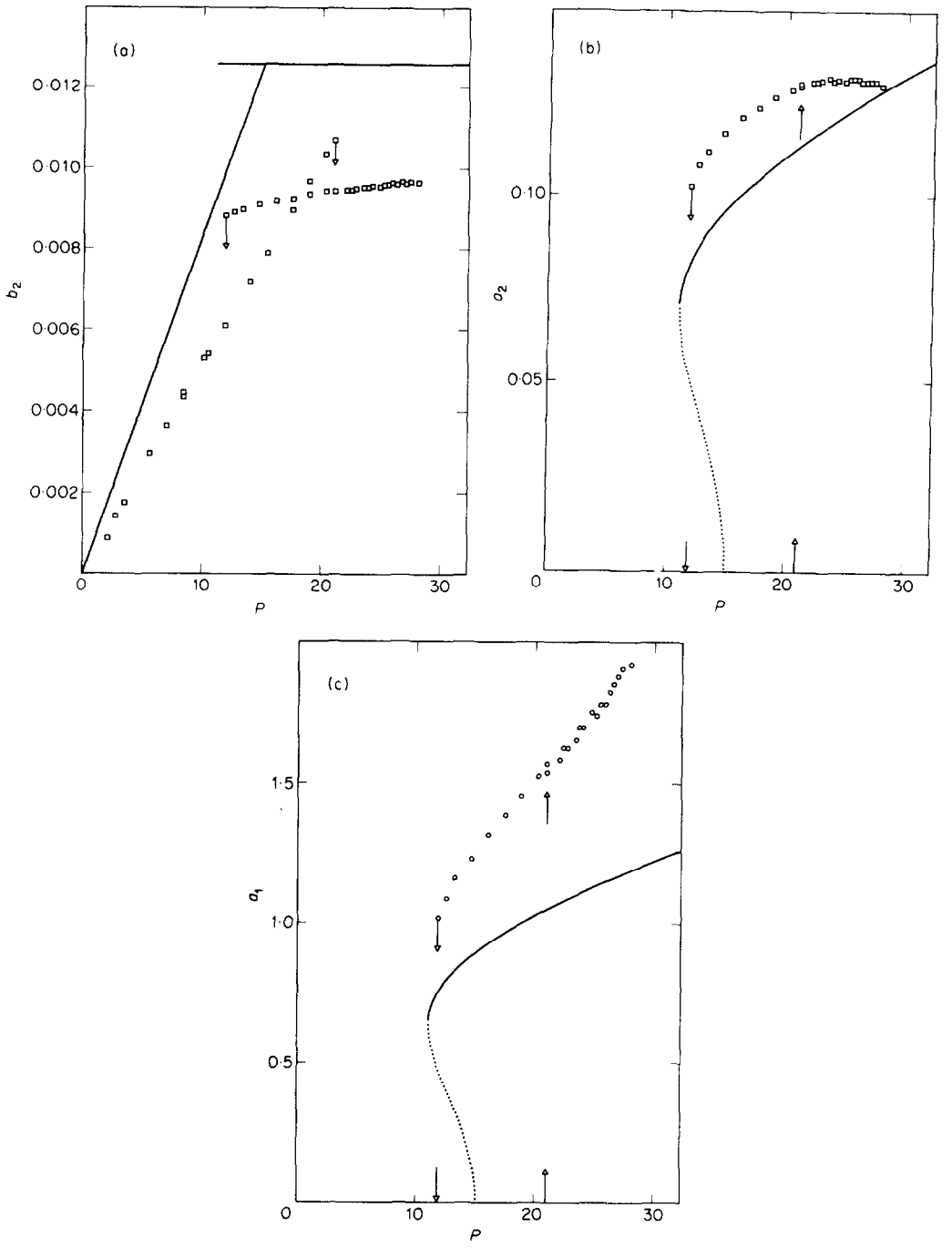

Figure 7. Effect of excitation parameter P on system three-mode interactive response, under internal resonance condition. $\varepsilon = 0{\cdot}075$, $\sigma = 10{\cdot}6$, $\sigma_1 = 5{\cdot}3$, $\zeta_B = 0{\cdot}04$, $\zeta_T = 0{\cdot}03$, $\zeta_2 = 0{\cdot}27$. (a) Planar second bending mode; (b) first torsional mode; (c) first non-planar bending mode. ——, Theory; ⊡, experiment.

response. It is indicated on the graphs that in this region responses were multi-harmonic and non-stationary. Further work is required to explore these regions.

Typical system responses for varying excitation amplitude P with other parameters held constant are shown in Figures 7(a)-(c). A test run starts from a small value of P

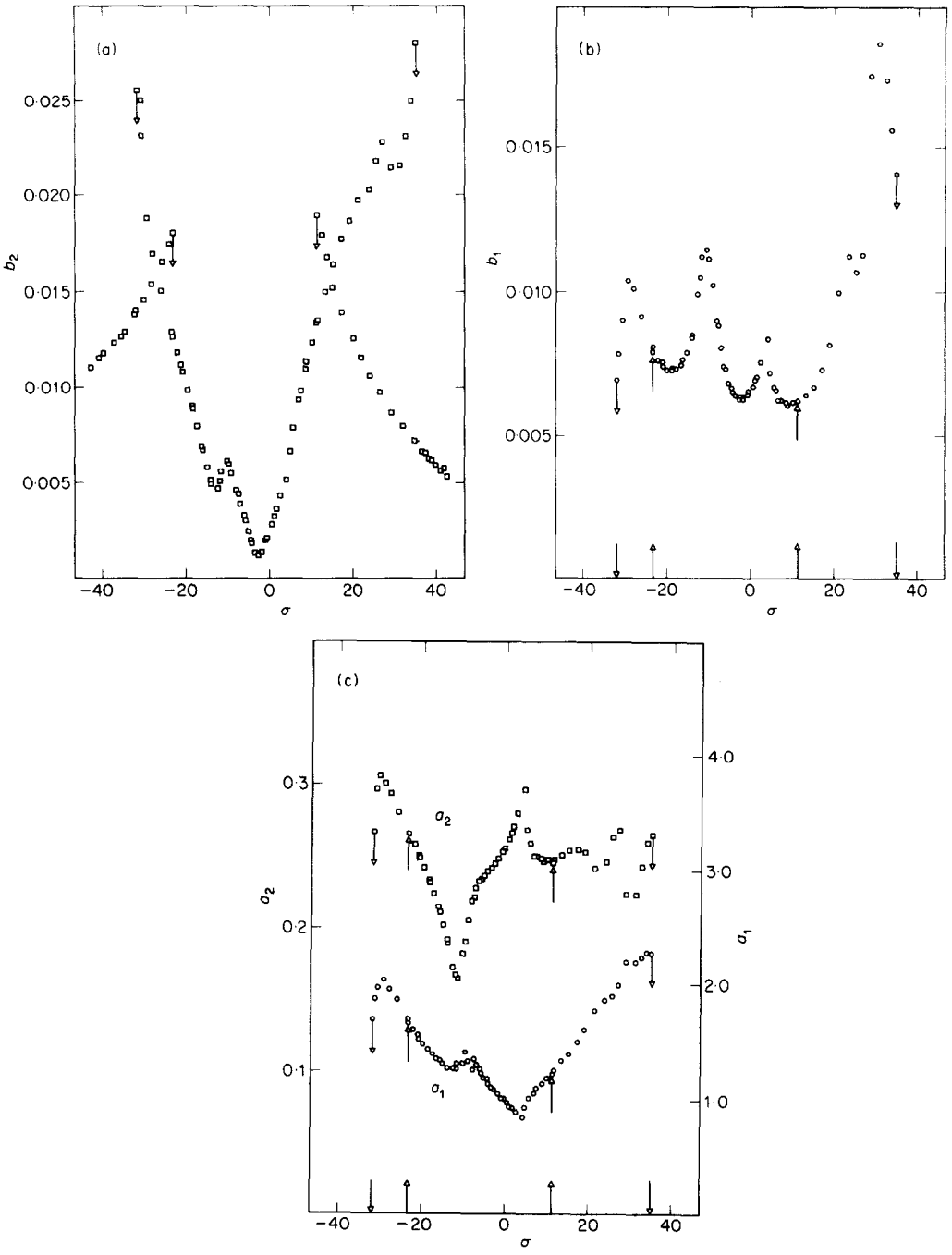

Figure 8. System four-mode interactive motions under multiple internal resonance. Measured response amplitudes as functions of external detuning parameter σ. $\varepsilon = 0{\cdot}075$, $P = 66$, $\sigma_1 = -22{\cdot}6$, $\sigma_2 = 0$, $\zeta_B = 0{\cdot}04$, $\zeta_T = 0{\cdot}03$, $\zeta_1 = 0{\cdot}13$, $\zeta_2 = 0{\cdot}27$. (a) Planar second bending mode; (b) planar first bending mode; (c) non-planar first bending mode (a_1) and first torsional mode (a_2).

which is then increased up to the critical value when there is an onset autoparametric interaction. P is further increased to some upper value, after which it is slowly decreased to zero. The threshold value of P at which autoparametric interaction begins is revealed by upward "jump" arrows for a_1 and a_2, and a downward "jump" arrow for b_2. For the

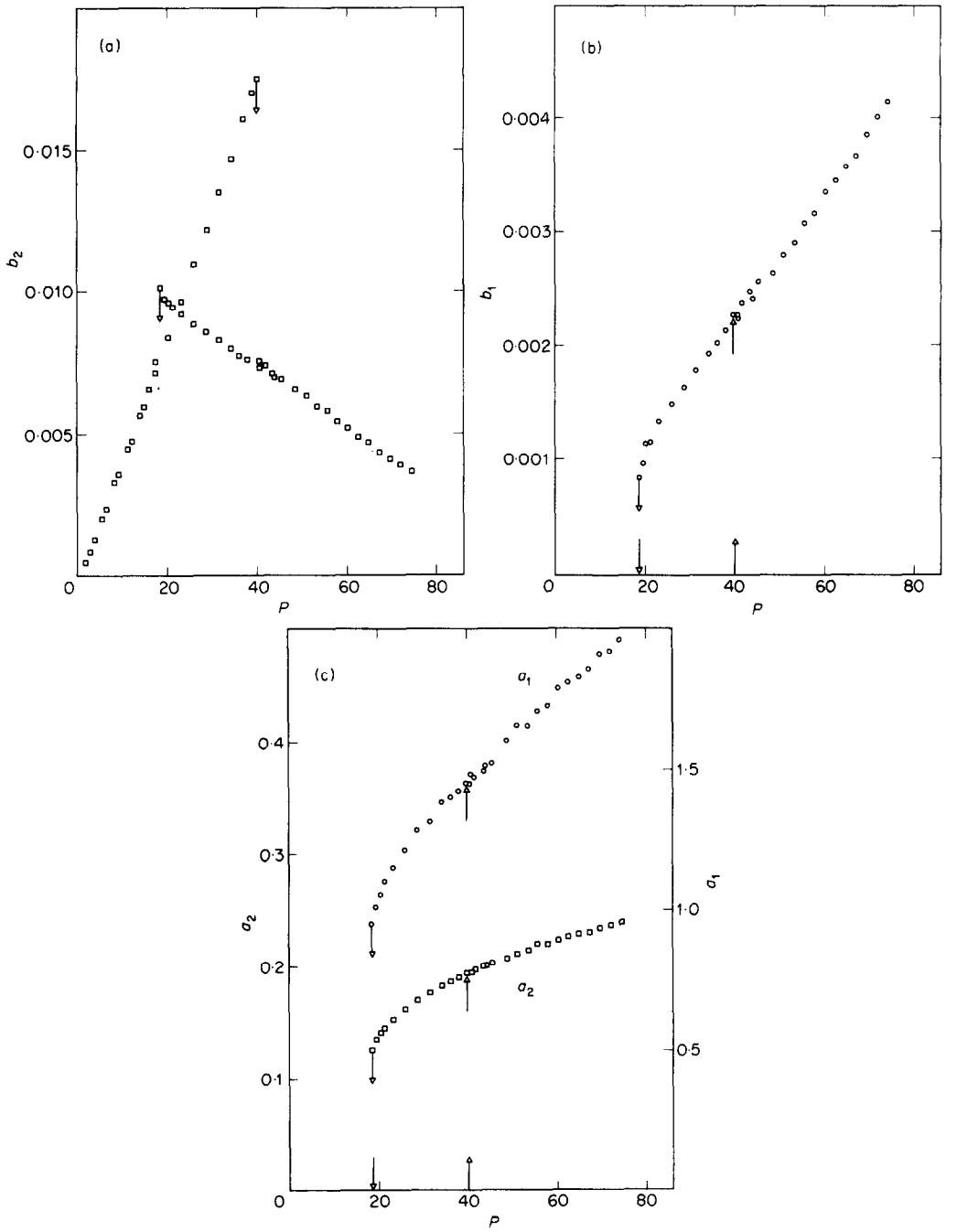

Figure 9. System four-mode interactive motion under multiple internal resonance. Measured response amplitudes as functions of excitation parameter P. $\varepsilon = 0{\cdot}075$, $\sigma = -13{\cdot}9$, $\sigma_1 = -18{\cdot}1$, $\sigma_2 = 6{\cdot}4$, $\zeta_B = 0{\cdot}04$, $\zeta_T = 0{\cdot}03$, $\zeta_1 = 0{\cdot}13$, $\zeta_2 = 0{\cdot}27$. (a) Planar second bending mode; (b) planar first bending mode; (c) non-planar first bending mode (a_1) and first torsional mode (a_2).

case of P decreasing from its upper limit, a point is reached at which interaction stops, as shown by the downward "jump" arrows for b_2, a_2 and a_1.

The agreement between theory and experiments is most reasonable. The non-linear response of b_2 does not show the saturation effect exactly as predicted as there is generally

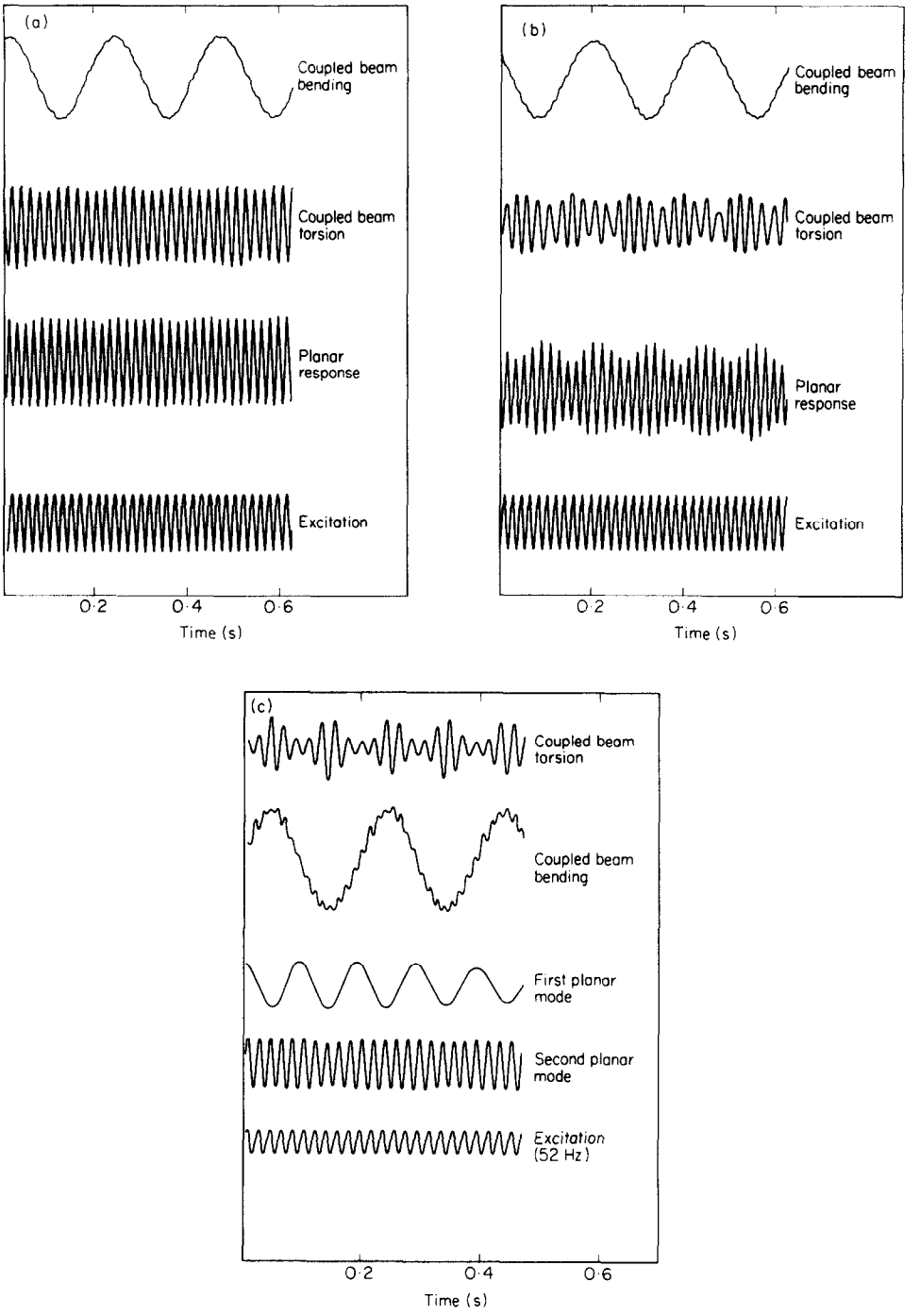

Figure 10. Time records of system interactive responses. (a) Three mode motion, excitation parameter $P = 3{\cdot}8$; (b) three-mode motion, excitation parameter $P = 15$; (c) four-mode interactive motion.

some small increase in b_2 with P. The measured values of a_2 and a_1 are generally higher than the predicted values and this discrepancy increases with P. The calculated values of the threshold value of P for the onset of autoparametric resonance are in all cases noticeably lower than the observed values.

4.4. FOUR-MODE INTERACTIVE MOTION

The three-mode internal resonance condition (38) was realizable over a sizeable range of tuning mass position, while within a small interval of that range the second internal resonance condition (50) could be achieved simultaneously. For this tuning condition violent interactive motions involving four modes were obtained when the external excitation frequency was resonant with the second in-plane mode at 52 Hz. Non-planar bending and torsional responses were present, and a first in-plane modal response at 9·5 Hz was discernible. A wide range of response characteristics was observed for variation of the three detuning parameters and excitation level. In this case, since only a qualitative explanation of the system behaviour is available from the analysis of sections 2.2 and 3.4 direct comparison with theory is not yet possible. The following graphs are presented as typical of the results obtained from the model and illustrate the essential features of the interactive responses.

Figures 8(a)-(c) show the response of the experimental model as the external detuning parameter σ is varied through the resonance region and show a region of interactive response of the first planar mode b_1. The upward jump arrows in Figures 8(b) and (c) indicate the transition points at which this non-linear resonance effect commences, while the downward jump arrows show the outer limits of existence of this phenomenon. The externally excited mode, response b_2 in Figure 8(a), is seen to exhibit a suppression effect as in the three-mode interaction problem. The remaining modes, on the other hand, show an irregular response pattern.

The model response as the force parameter P is varied is shown in Figures 9(a)-(c). The threshold value of P for the onset of this non-linear resonance behaviour is indicated by the upward jump arrows in Figures 9(b) and (c). When P is decreased from some upper limit, the responses of a_2, a_1 and b_1 show a substantial hysteresis effect, as indicated by the positions of the downward jump arrows.

Finally, Figures 10(a)-(c) show some typical time records obtained from transducers under various conditions. These reveal the complex non-synchronous nature of the interactive responses. Figures 10(a) and (b) represent three-mode coupling at low and high levels of excitation parameter P and show the change from reasonably stationary to non-stationary response. Figure 10(c) represents four-mode coupling and indicates clearly the large spread of frequency of the simultaneous responses.

5. CONCLUSIONS

Violent non-linear interactive vibration involving planar bending modes and two non-planar bending and torsional modes, observed to occur in a specific form of coupled beam system, has been investigated theoretically and experimentally. Perturbation analysis conducted to first order revealed that the complex responses were due to the occurrence of one, or two, internal resonances. In the case of the single internal resonance of summed type a stationary solution was obtained for the three-mode interactive response under forced vibration. Comparison with experimental tests showed extremely reasonable agreement with the predicted responses.

For the more complicated case of four-mode interactive response in the presence of two simultaneous internal resonances, a qualitative explanation of the phenomenon was

given and the system equations were reduced to an autonomous set of first order equations. No stationary solutions were obtained in this case. Some experimental results were presented to illustrate the complex response patterns obtained in this case. Although a specific and restricted structural form has been investigated, it must be expected that similar or closely related response phenomena will occur in more complicated structural arrangements under conditions of high excitation and low damping, and that due account must be taken of such internal resonance effects as sources of enhanced vibratory response.

ACKNOWLEDGMENT

The studentship awarded to one of the authors (S.L.B.) by the University of Edinburgh during the course of this research is gratefully acknowledged.

REFERENCES

1. J. W. ROBERTS 1980 *Journal of Sound and Vibration* **69**, 101–116. Random excitation of a vibratory system with autoparametric interaction.
2. V. V. BOLOTIN 1964 *The Dynamic Stability of Elastic Systems.* San Francisco: Holden-Day.
3. J. DUGUNDJI and V. MUKHOPADHYAY 1973 *Journal of Applied Mechanics* **40**, 693–698. Lateral bending-torsion vibrations of a thin beam under parametric excitation.
4. E. DOKUMACI 1978 *Journal of Sound and Vibration* **58**, 233–238. Pseudo-coupled bending-torsion vibrations of beams under lateral parametric excitation.
5. E. BREITENBERGER and R. D. MUELLER 1981 *Journal of Mathematical Physics* **22**, 1196–1210. The elastic pendulum: a non-linear paradigm.
6. P. R. SETHNA 1965 *Journal of Applied Mechanics* **32**, 576–582. Vibrations of dynamical systems with quadratic non-linearities.
7. T. YAMAMOTO and K. YASUDA 1977 *Bulletin of the Japanese Society of Mechanical Engineers* **20**, 168–175. On the internaal resonance in a non-linear two-degree-of-freedom system (Forced vibrations near the lower resonance point when the natural frequencies are in the ratio 1:2).
8. T. YAMAMOTO, K. YASUDA and I. NAGASAKA 1977 *Bulletin of the Japanese Society of Mechanical Engineers* **20**, 1093–1100. On the internal resonance in a two-degree-of-freedom system (Forced vibrations near the higher resonance point when the natural frequencies are in the ratio 1:2).
9. T. YAMAMOTO, K. YASUDA and I. NAGASAKA 1979 *Bulletin of the Japanese Society of Mechanical Engineers* **22**, 1274–1283. On the internal resonance in a non-linear two-degree-of-freedom system (When the natural frequencies are in the ratio 2:3).
10. P. R. SETHNA and A. K. BAJAJ 1978 *Journal of Applied Mechanics* **45**, 895–902. Bifurcations in dynamical systems with internal resonance.
11. R. S. HAXTON and A. D. S. BARR 1972 *Journal of Engineering for Industry* **94**, 119–125. The autoparametric vibration absorber.
12. A. D. S. BARR and D. J. NELSON 1972 *Symposium on Non-linear Dynamics, Loughborough University of Technology.* Autoparametric interaction in structures.
13. A. H. NAYFEH, D. T. MOOK and L. R. MARSHALL 1973 *Journal of Hydronautics* **7**, 145–152. Non-linear coupling of pitch and roll modes in ship motions.
14. D. T. MOOK, L. R. MARSHALL and A. H. NAYFEH 1974 *Journal of Hydronautics* **8**, 32–40. Subharmonic and superharmonic resonances in the pitch and roll modes of ship motions.
15. R. A. IBRAHIM and A. D. S. BARR 1975 *Journal of Sound and Vibration* **42**, 159–179. Autoparametric resonance in a structure containing a liquid, Part I: Two mode interaction.
16. R. A. IBRAHIM and A. D. S. BARR 1975 *Journal of Sound and Vibration* **42**, 181–200. Autoparametric resonance in a structure containing a liquid, Part II: Three mode interaction.
17. N. YEN and R. E. KRONAUER 1977 *Journal of Applied Mechanics* **44**, 141–146. Response of three oscillators coupled by a weak non-linearity.
18. J. W. KLAHS, JR and J. H. GINSBERG 1979 *Journal of Applied Mechanics* **46**, 132–139. Resonant excitation of a spinning nutating plate.
19. H. HATWAL, A. K. MALLIK and A. GHOSH 1982 *Journal of Sound and Vibration* **81**, 153–164. Non-linear vibrations of harmonically excited autoparametric system.

20. A. D. S. BARR 1980 *Proceedings of the International Conference on Recent Advances in Structural Dynamics, Southampton University.* Some developments in parametric instability and non-linear vibration.
21. R. A. IBRAHIM 1976 *Journal of Engineering for Industry* **98**, 1092–1098. Multiple internal resonance in a structure-liquid system.
22. A. D. S. BARR and R. P. ASHWORTH 1976 *U.S. Air Force Office of Scientific Research, Washington D.C., Report AFOSR* 74-2723. Parametric and non-linear mode interaction behaviour in the dynamics of structures.
23. A. H. NAYFEH 1973 *Perturbation Methods.* New York: Wiley-Interscience.
24. A. H. NAYFEH and D. T. MOOK 1979 *Non-linear Oscillations.* New York: Wiley-Interscience.
25. D. A. PETERS and R. A. ORMISTON 1973 *Journal of the American Helicopter Society* **18**, 45–48. The effects of second order blade bending on the angle of attack of hingeless rotor blades.
26. S. L. BUX 1983 *Ph.D. Thesis, University of Edinburgh.* Vibrations of coupled beam systems with non-linear interactions.

APPENDIX I

Specification of integrals for the coefficients of the system equations of motion:

$$\lambda_1 = EI_{yy}\int_0^l [f''(z)]^2\,dz, \qquad \lambda_2 = GJ\int_0^l [g'(z)]^2\,dz, \tag{A1, A2}$$

$$\lambda_3 = \int_0^l [f'(z)]^2\,dz, \qquad \lambda_4 = \int_0^l (l-z)f''(z)g(z)\,dz. \tag{A3, A4}$$

APPENDIX II

Elements of the matrix for the linearized system for perturbation of the stationary solutions are as follows:

$$C_{11} = -\zeta_B\omega_B, \quad C_{21} = \sqrt{\zeta_B\zeta_T}\,\omega_B, \quad C_{12} = \sqrt{\zeta_B\zeta_T}\,\omega_T, \quad C_{22} = -\zeta_T\omega_T,$$

$$C_{13} = \zeta_B\omega_B a_{10}/b_{20}, \quad C_{23} = \sqrt{\zeta_B\zeta_T}\,\omega_B a_{10}/b_{20}, \quad C_{14} = 0, \quad C_{24} = 0,$$

$$C_{15} = -\zeta_B\omega_B\kappa_{22}a_{10}, \quad C_{25} = -\sqrt{\zeta_B\zeta_T}\,\omega_B\kappa_{22}a_{10}, \quad C_{31} = -\zeta_B\omega_B^2K_1a_{10}/b_{20},$$

$$C_{32} = -\sqrt{\zeta_B\zeta_T}\,\omega_B\omega_TK_1a_{10}/b_{20}, \quad C_{33} = -\zeta_2\omega_2, \quad C_{34} = -\sigma b_{20} + \zeta_B\omega_B^2K_1K_2a_{10}^2/b_{20},$$

$$C_{35} = \zeta_B\omega_B^2\kappa_{11}\kappa_{22}a_{10}^2/b_{20}, \quad C_{41} = -\zeta_B\omega_B^2\kappa_{11}\kappa_{22}a_{10}/b_{20}^2,$$

$$C_{42} = -\sqrt{\zeta_B\zeta_T}\,\omega_B\omega_TK_1K_2a_{10}/b_{20}^2, \quad C_{43} = -\sigma/b_{20},$$

$$C_{44} = -\zeta_2\omega_2 + \zeta_B\omega_B^2K_1a_{10}^2/b_{20}^2, \quad C_{45} = -\zeta_B\omega_B^2K_1a_{10}^2/b_{20}^2,$$

$$C_{51} = -C_{41} - (\zeta_T\omega_T - \zeta_B\omega_B)K_2/a_{10}, \quad C_{52} = -C_{42} - (\zeta_B\omega_B - \zeta_T\omega_T)\sqrt{\zeta_T}\,\omega_TK_2/\sqrt{\zeta_B}\,\omega_Ba_{10},$$

$$C_{53} = -(2\sigma + \sigma_1)/b_{20}, \quad C_{54} = -C_{44}, \quad C_{55} = -C_{45} - (\zeta_B\omega_B + \zeta_T\omega_T).$$

Here $K_1 = \mu_2(\omega_B + \omega_T)^2/\kappa_{22}\omega_2^3$ and $K_2 = (\sigma + \sigma_1)/(\zeta_B\omega_B + \zeta_T\omega_T)$.